Tight-binding theory of the electronic structures for rhombohedral semimetals

J. H. Xu
Department of Physics and Texas Center for Superconductivity, University of Houston, Houston, Texas 77204

E. G. Wang
Space Vacuum Epitaxy Center, University of Houston, Houston, Texas 77204

C. S. Ting
Department of Physics and Texas Center for Superconductivity, University of Houston, Houston, Texas 77204

W. P. Su
Department of Physics and Texas Center for Superconductivity, University of Houston, Houston, Texas 77204 and Space Vacuum Epitaxy Center, University of Houston, Houston, Texas 77204

(Received 2 June 1993; revised manuscript received 20 August 1993)

A semiempirical tight-binding theory of energy bands in rhombohedral $A7$-structure crystals is developed and applied to three group-V semimetals: arsenic, antimony, and bismuth. A general description of the method is explicitly given, including the matrix elements of the tight-binding Hamiltonian, and the treatment of the spin-orbit interaction which is noticeable in Bi. For each of these materials the theory uses 15 parameters, obtained in accord with a third-neighbor model which includes the spin-orbit coupling, to reproduce the major features of the band structures. The determination of these parameters is made by fitting the existing pseudopotential and *ab initio* data for the band structures at some high-symmetry points of the Brillouin zone. Comparison with first-principle calculations and experiments gives very good agreement throughout.

I. INTRODUCTION

Recent experiments have demonstrated that an antimony layer can be grown on a GaSb substrate along the (111) direction by the molecular-beam epitaxy (MBE) technique.[1] The Bi/CdTe (111) heterostructures have been also successfully fabricated.[2] Bulk Sb and Bi are group-V semimetals with equal numbers of electrons and holes. Their conduction-band minima (at the L point) lie at a lower energy than the valence-band maxima (at the H point in Sb, at the T point in Bi). The overlap of the two bands is ≈ 180 meV in Sb and ≈ 40 meV in Bi.[3] Both Sb and Bi have large characteristic lengths: the mean free path is a few micrometers and the de Broglie wavelength is of 400 Å. Consequently the interesting quantum size effect is expected if the carriers in these semimetals are spacially confined. Such confinement can be achieved by sandwiching the semimetal film between layers of a suitable barrier material. When the thickness of the semimetal film decreases, the electron subbands should move up in energy while the hole subbands move down. At a certain thickness, the electron and hole subbands will cross and a semimetal-semiconductor transition occurs. It has recently been suggested that a narrow-gap semiconductor whose band alignment is indirect in momentum space would have highly attractive properties in optical and electro-optical device application.[4] Indirect narrow-gap heterostructures such as Sb/GaSb (111) and Bi/CdTe (111) superlattices could potentially open a new possibility in device manufacture. This situation will put new demands on theorists to predict the properties of exotic semiconductor-semimetal heterostructures before the materials are even fabricated. Thus we need an effectively theoretial method to survey and simulate very complicated semimetal materials. Such an approach should allow a rapid scan of many different electronic properties for a complicated system. The semiempirical tight-binding theory possesses such an advantage, and has been widely used to calculate the band structures in diamond and zinc-blende semiconductors[5–8] and their heterostructures.[9] The results obtained from this method have often been compared successfully with corresponding experimental data. The rhombohedral $A7$ semimetals and their heterostructures have not received similar attention up to now. At this moment, a comparable tight-binding theory for the rhombohedral $A7$ structure semimetals and their heterostructures is highly needed.

From a theoretical point of view, a lot of band-structure and total-energy calculations for As, Sb, and Bi have been carried out. We can mention an early oversimplified tight-binding calculation for bismuth,[10] the qualitative analysis of binding in group-V rhombohedral compounds,[11] the pseudopotential calculations,[12–14] and the *ab initio* studies[15] of As, Sb, and Bi. A systematic tight-binding theory, comparable to that developed for zinc-blende and diamond semiconductors, has not been tried until recently because of the complications arising from the relatively low symmetry of the rhombohedral $A7$ structure. However, the theoretical simulation of the complicated systems such as rhombohedral semimetals and their heterostructures depends greatly on a reliable tight-binding approach.

0163-1829/93/48(23)/17271(9)/$06.00

The purpose of this paper is to present such a theory for bulk rhombohedral crystals. We show that a tight-binding method using a few interaction parameters gives accurate results for the band structures. We hope that the tight-binding parameters determined in the present work can be used to calculate the electronic properties of the semimetal-semiconductor superlattices and heterostructures.

The tight-binding method we use is equivalent to that of Slater and Koster.[5] It can also be regarded as a more complete version of the Weaire and Thorpe model[16] in which interactions between more distant directed orbitals are included. It is necessary to include these extra interactions for a more complete description of the fine structures in the energy bands. Our model has the following properties. (i) The chemistry of s^2p^3 bonding is manifestly preserved. This is because the external electron configuration of As, Sb, and Bi is s^2p^3, plus a complete d shell. Those s and p levels will mix in the solid, while the other d electron and core-electron levels will remain practically unchanged. This means that only the five s and p electrons will be considered as valence electrons, while the others will be considered as being part of the ionic core. (ii) The spin-orbit interaction is included in the theory. Each energy level of p electrons will split into two levels due to the spin-orbit coupling. The amplitude of the splitting increases with the element atomic number: approximately 0.36 eV for As, 0.6 eV for Sb, and 1.5 eV for Bi.[12,17] In the case of As and Sb, this coupling leads to the suppression of several specific degeneracies, which can be observed in the band structure, with little influence on the global electronic properties. In the case of bismuth, however, the effect turns out to be significant. (iii) the theory successfully reproduces not only the valence bands but also the lower conduction bands, even in indirect (negative) gap semimetals.

In Sec. II, we discuss the rhombohedral $A7$ structure; the tight-binding Hamiltonian is given in Sec. III; and the resulting band structures for As, Sb, and Bi are presented in Sec. IV. Section V includes conclusion and discussions. The explicit expressions of the tight-binding matrix elements are given in the Appendix.

II. RHOMBOHEDRAL $A7$ STRUCTURE

The typical structure of group-V elements is the rhombohedral $A7$ structure. It is the common cyrstal phase of As, Sb, and Bi. The $A7$ structure can be viewed as a distortion of simple cubic. It can be obtained from simple cubic by a strain of the unit cell along the (111) direction and a simultaneous displacement of the atoms of the basis towards each other in pairs along the same direction. The resulting lattice, which has trigonal symmetry and two atoms per unit cell,[18] is shown in Fig. 1. Under these distortions the six nearest neighbors of each atom of the simple cubic structure distort to become three nearest and three next-nearest neighbors. This can be understood in terms of chemical bonds, since the group-V elements preferentially form three bonds.[19] The primitive translation vectors of the lattice can be expressed by

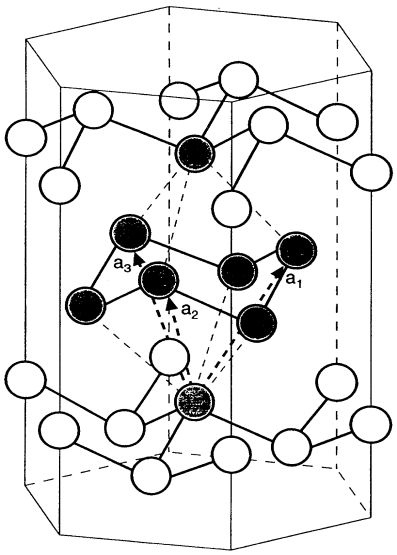

FIG. 1. Rhombohedral $A7$ structure.

$$\begin{aligned}\mathbf{a}_1&=(-\sqrt{3}/6,-1/2,c_1+c_2)a\ ,\\ \mathbf{a}_2&=(\sqrt{3}/3,0,c_1+c_2)a\ ,\\ \mathbf{a}_3&=(-\sqrt{3}/6,1/2,c_1+c_2)a\ .\end{aligned}\tag{2.1}$$

The values of a, c_1, and c_2 for As, Sb, and Bi are listed in Table I.[20–22] The parameters c_1 and c_2 are related to the shear angle α and the bond length a_{nn} (the nearest-neighbor distance) by

$$c_1=\left[\left[\frac{a_{nn}}{a}\right]^2-\frac{1}{3}\right]^{1/2},\tag{2.2}$$

$$c_2=\frac{\left[1-\frac{4}{3}\sin^2\frac{\alpha}{2}\right]^{1/2}}{2\sin\frac{\alpha}{2}}-c_1\ .\tag{2.3}$$

Each point in the reciprocal lattice is specified by a vector $\mathbf{l}=l_1\mathbf{b}_1+l_2\mathbf{b}_2+l_3\mathbf{b}_3$ where the three reciprocal-lattice vectors $\mathbf{b}_i$ with $i=1$, 2, and 3 are defined by $\mathbf{b}_i\cdot\mathbf{a}_j=2\pi\delta_{ij}$, and l_1 l_2, and l_3 are integers. In the rectangular coordinate systems, we have

TABLE I. Crystal structure parameters of As, Sb, and Bi.

	As	Sb	Bi
a	3.7597 Å	4.3084 Å	4.5332 Å
c	10.442 Å	11.274 Å	11.800 Å
a_{nn}	2.5165 Å	2.9080 Å	3.0624 Å
α	54.554°	57.11°	57.35°
c_1	1.2731 Å	1.5065 Å	1.5896 Å
c_2	2.2074 Å	2.2513 Å	2.3426 Å

$$l=b\left[\sin\varphi\left[l_2-\frac{l_1+l_3}{2}\right],\frac{\sqrt{3}}{2}\sin\varphi(l_3-l_1),\cos\varphi(l_1+l_2+l_3)\right], \tag{2.4}$$

where $\cos\varphi=(\sqrt{3}/3)\tan(\alpha/2)$. From the above relation it follows that

$$|l|^2=b^2[l_1^2+l_2^2+l_3^2+\cos\beta(l_1l_2+l_2l_3+l_3l_1)], \tag{2.5}$$

where β, the angle between any two reciprocal vectors, is related to the shear angle α by

$$\cos\beta=-\frac{\cos\alpha}{1+\cos\alpha}. \tag{2.6}$$

Thus, the equation of any face of the Brillouin zone in rectangular coordinates can be obtained by using Eq. (2.5) with the relation $\mathbf{k}\cdot l=\frac{1}{2}|l|^2$. Figure 2 represents the first Brillouin zone; the usual notation for symmetry points has been used.[20]

III. MODEL HAMILTONIAN

In rhombohedral $A7$ structure crystals, there are two atoms in the primitive cell. If we neglect the spin-orbit interaction for each tight-binding basis function centered on these atoms, two Bloch functions can be constructed:

$$|n,\alpha,\mathbf{k}\rangle=\frac{1}{\sqrt{N}}\sum_i e^{i\mathbf{k}\cdot\mathbf{R}_i+i\mathbf{k}\cdot\mathbf{r}_\alpha}|n,\alpha,\mathbf{R}_i\rangle. \tag{3.1}$$

The quantum number n runs over the s, p_x, p_y, and p_z orbitals. The N wave vectors $\mathbf{k}$ lie in the first Brillouin zone; the site index α is either 1 or 2. The atom 1 is located at $\mathbf{R}_i$. The tight-binding basis functions $|n,\alpha,\mathbf{R}_i\rangle$ are Löwdin orbitals: i.e., the symmetrically orthogonalized atomic orbitals.[23]

The Schrödinger equation for the Bloch function $|\mathbf{k},\lambda\rangle$ is

$$[H-E_\lambda(k)]|\mathbf{k},\lambda\rangle=0, \tag{3.2}$$

or, in this basis,

$$\sum_{n',\alpha'}[\langle n,\alpha,\mathbf{k}|H|n',\alpha',\mathbf{k}\rangle-E_\lambda(k)\delta_{nn'}\delta_{\alpha\alpha'}]\langle n',\alpha',\mathbf{k}|\mathbf{k},\lambda\rangle=0. \tag{3.3}$$

The solutios are

$$|\mathbf{k},\lambda\rangle=\sum_{n,\alpha}\langle n,\alpha,\mathbf{k}|\mathbf{k},\lambda\rangle|n,\alpha,\mathbf{k}\rangle. \tag{3.4}$$

The band index λ has eight values. The basis problem of the tight-binding method is to find the matrix elements of Hamiltonian between the various basis states. In the semimetals As, Sb, and Bi, we consider only one set of s, p_x, p_y, and p_z orbitals at each atom. We will denote these by s_1, p_{x1}, p_{y1}, p_{z1}, or s_2, p_{x2}, p_{y2}, p_{z2}, where the subscripts refer to the atoms in the unit cell. The Hamiltonian matrix in the $|n,\alpha,\mathbf{k}\rangle$ representing all possible nearest-neighbor, next-nearest-neighbor, and third-nearest neighbor interactions between the tight-binding basis functions centered on each atom in the crystal can be calculated from the Slater and Koster approach,[5]

$$H_{\alpha\alpha'}(\mathbf{k})=\sum_i e^{i\mathbf{k}\cdot\mathbf{r}_i}\langle 0,\alpha|H|i,\alpha'\rangle. \tag{3.5}$$

For each atom in the unit cell there are three nearest neighbors, three next-nearest neighbors, and six third-nearest neighbors as shown in Fig. 1. Now we need the atomic matrix elements $\langle 0,\alpha|H|i,\alpha'\rangle$, the form of which has been given by Slater and Koster.[5] Chadi and Cohen[7] have reported the (8×8) secular determinant for diamond and zinc-blende crystals. Later on Vogl, Hjalmarson, and Dow[8] extended this approach to the sp^3s^* basis for the zinc-blende semiconductors. Here we give the Hamiltonian matrix on the sp^3 basis for rhombohedral $A7$ structure semimetals:

	s_1	p_{x1}	p_{y1}	p_{z1}	s_2	p_{x2}	p_{y2}	p_{x2}
s_1	H_{1s1s}	H_{1s1x}	H_{1s1y}	0	H_{1s2s}	H_{1s2x}	H_{1s2y}	H_{1s2z}
p_{x1}	H^*_{1s1x}	H_{1x1x}	H_{1x1y}	0	$-H_{1s2x}$	H_{1x2x}	H_{1x2y}	H_{1x2z}
p_{y1}	H^*_{1s1y}	H^*_{1x1y}	H_{1y1y}	0	$-H_{1s2y}$	H_{1x2y}	H_{1y2y}	H_{1y2z}
p_{z1}	0	0	0	H_{1z1z}	$-H_{1s2z}$	H_{1x2x}	H_{1y2z}	H_{1z2z}
s_2	H^*_{1s2s}	$-H^*_{1s2x}$	$-H^*_{1s2y}$	$-H^*_{1s2z}$	H_{1s1s}	H_{1s1x}	H_{1s1y}	0
p_{x2}	H^*_{1s2x}	H^*_{1x2x}	H^*_{1x2y}	H^*_{1x2z}	H^*_{1s1x}	H_{1x1x}	H_{1x1y}	0
p_{y2}	H^*_{1s2y}	H^*_{1y2z}	H^*_{1y2y}	H^*_{1x2z}	H^*_{1s1y}	H^*_{1x1y}	H_{1y1y}	0
p_{z2}	H^*_{1s2z}	H^*_{1x2z}	H^*_{1y2z}	H^*_{1z2z}	0	0	0	H_{1z1z}

The explicit expressions of these matrix elements are given in Appendix. In Eqs. (A1)–(A17) there are fourteen interaction parameters to be determined: E_s, E_p, $V_{ss\sigma}$, $V_{sp\sigma}$, $V_{pp\pi}$, $V_{pp\sigma}$, $V'_{ss\sigma}$, $V'_{sp\sigma}$, $V'_{pp\pi}$, $V'_{pp\sigma}$, $V''_{ss\sigma}$, $V''_{sp\sigma}$, $V''_{pp\pi}$, and $V''_{pp\sigma}$. The first two are the on-site orbital energies. The third to sixth and seventh to tenth are the nearest-neighbor and next-nearest-neighbor interaction parameters. The last four are the third-neighbor interac-

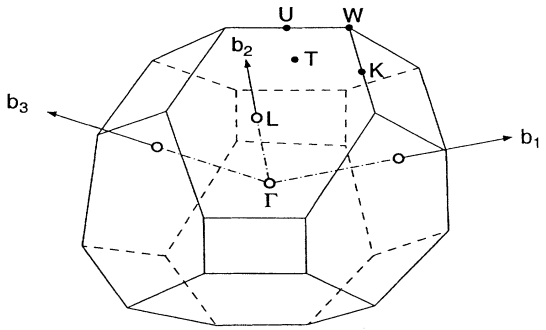

FIG. 2. Brillouin zone for rhombohedral $A7$ crystals.

tion parameters. Here the two-center approximation has been used.

From Eqs. (A1)–(A17) we can see that our Hamiltonian matrix elements are much more complicated than those given by Chadi and Cohen[7] and Vogl, Hjalmarson, and Dow[8] for zinc-blende and diamond semiconductors because the rhombohedral $A7$ crystals have the relatively low symmetry.

In order to obtain the interaction parameters we will use the dependence of the energy levels (at a few points in the Brillouin zone) on the potentials. Along some symmery lines and at some symmetry points the dependence of the energies on the interaction parameters can be obtained in closed form. Here we list some of these relations.

At the Γ point, the doubly degenerate eigenvalues are given by

$$E(\Gamma_{45}^{\pm})=E_p+3(V''_{pp\sigma}+V''_{pp\pi})\pm\tfrac{3}{2}(V_{pp\sigma}A_1^2+V'_{pp\sigma}A_2^2) \pm 3[V_{pp\pi}(1-\tfrac{1}{2}A_1^2)+V'_{pp\pi}(1-\tfrac{1}{2}A_2^2)] , \quad (3.6)$$

where A_1 and A_2 are defined by Eq. (A20) in the Appendix. If we set the s-p interaction parameters $V'_{sp\sigma}=\sqrt{(1-A_1^2)/(1-A_2^2)}V_{sp\sigma}$, we have

$$E(\Gamma_6^{\pm})=E_s+6V''_{ss\sigma}\pm 3(V_{ss\sigma}+V'_{ss\sigma}) , \quad (3.7)$$

$$E(\Gamma_6'^{\pm})=E_p+3(V''_{pp\sigma}+V''_{pp\pi})\pm 3(V_{pp\pi}A_1^2+V'_{pp\pi}A_2^2) \pm 3[V_{pp\sigma}(1-A_1^2)+V'_{pp\sigma}(1-A_2^2)] . \quad (3.8)$$

Along the Γ-T-L and T-H directions, only the energies of the nondegenerate bands can be obtained in closed form:

$$E=E_p+V''_{pp\sigma}\left[2+\cos\frac{\sqrt{3}}{2}k_x\right]+3V''_{pp\pi}\cos\frac{\sqrt{3}}{2}k_x \pm\left\{\alpha^2+\beta^2+V_{pp\pi}^2+V_{pp\pi}'^2+2(\alpha V_{pp\pi}+\beta V'_{pp\pi})\cos\frac{\sqrt{3}}{2}k_x+2\alpha\beta\cos\left[\frac{\sqrt{3}}{3}k_x+(c_1+c_2)k_z\right] +2(\alpha V'_{pp\pi}+\beta V_{pp\pi})\cos\left[\frac{\sqrt{3}}{6}k_x-(c_1+c_2)k_z\right]+2V_{pp\pi}V'_{pp\pi}\cos\left[\frac{\sqrt{3}}{3}k_x-(c_1+c_2)k_z\right]\right\}^{1/2} , \quad (3.9)$$

where

$$\alpha=\tfrac{3}{2}V_{pp\sigma}A_1^2+2V_{pp\pi}(1-\tfrac{3}{4}A_1^2) , \quad (3.10)$$

$$\beta=\tfrac{3}{2}V'_{pp\sigma}A_2^2+2V'_{pp\pi}(1-\tfrac{3}{4}A_2^2) . \quad (3.11)$$

IV. BAND STRUCTURES OF RHOMBOHEDRAL SEMIMETALS

With the help of the relations between energies and potentials given in the preceding section [see Eqs. (3.6)–(3.9)], the empirical matrix elements of the sp^3 Hamiltonian can be obtained by fitting the pseudopotential[12–14] and *ab initio*[15] results. Before doing this, we should point out here that the spin-orbit interaction plays an important role in determining the electronic band structure for group-V semimetals. Going from As to Sb to Bi, the strength of the spin-orbit interaction increases. The spin-orbit coupling parameters λ for p^3 electron configuration are of the order of 0.3 eV for As, 0.6 eV for Sb, and 1.5 eV for Bi,[12,17] respectively, which are almost the same order of magnitude as the nearest-neighbor interaction integrals. The spin-orbit component of the Hamiltonian

$$H_{\text{s.o.}}=\frac{\hbar^2}{4m^2c^2}(\nabla V\times\mathbf{k})\cdot\sigma , \quad (4.1)$$

where V is the total crystal potential and σ represents the Pauli spin matrix, couples p orbitals on the same atom. In this case we should take $(s\alpha)_i$, $(s\beta)_i$, $(p_x\alpha)_i$, $(p_x\beta)_i$, $(p_y\alpha)_i$, $(p_y\beta)_i$, $(p_z\alpha)_i$, and $(p_z\beta)_i$ (where $i=1,2$, and α,β denote spin states) as basis functions and extend the dimension of the tight-binding Hamiltonian matrix from (8×8) to (16×16).

In order to calculate the matrix elements of $H_{\text{s.o.}}$, we note that our basis functions can be expressed in terms of $|j,m\rangle$, the eigenfunctions of the total angular momentum. Then, the spin-orbit coupling parameter λ can be defined as the split between triplet and singlet states on the basis of the total angular momentum:

$$\lambda=(4\pi/3)(\langle\tfrac{3}{2},m|H_{\text{s.o.}}|\tfrac{3}{2},m\rangle-\langle\tfrac{1}{2},m|H_{\text{s.o.}}|\tfrac{1}{2},m\rangle) . \quad (4.2)$$

The tight-binding parameters for As, Sb, and Bi obtained by fitting the pseudopotential[12–14] and *ab initio*[15] results are given in Table II. The values of spin-orbit coupling parameters λ we use here are 0.36 eV for As, 0.6 eV for Sb, and 1.5 eV for Bi. The resulting band structures are shown in Figs. 3–5, where the Fermi level is chosen as energy zero.

For As, it can be noted from Fig. 3 that the Fermi level crosses the band only near L and T, as well as H, which lie on the reflection plane σ of the Brillouin zone. In addition, the spin-orbit coupling leaves the degeneracy along the T-W line, leading to the minimum of the lowest conduction band being located at L, while the maxima of the valence band are at T and H. Our tight-banding calculation provides the correct location of the carriers, i.e., the electron pockets at the L point of the Brillouin zone and hole pockets at T and H. All these results are in good agreement with the pseudopotential[12] and the first-principle[15] results.

For Sb, one can see from Fig. 4 that the minimum of the lowest conduction band corresponds to L, while the maximum of the valence band is at H. We should point out here that if we neglect the spin-orbit coupling, there would be a crossover of two bands along the TW line; these two bands intersect the Fermi level very close to their crossover point. At first sight it would seem that that energy-level structure will give rise to extra electrons or extra holes, depending upon whether the crossover lies above or below the Fermi level. However, as is shown in Fig. 4, the spin-orbit interaction splits the conduction and valence bands at this point. In fact, the influeence of the spin-orbit coupling can be easily seen by means of a simple perturbation calculation. Let us consider the levels T_1 and T_2 in the neighborhood of the T point and assume a constant spin-orbit interaction λ. In this way, if the band energies $\epsilon_1(\mathbf{k})$ and $\epsilon_2(\mathbf{k})$ without spin-orbit coupling have a crossover along the T-W line, the total energies $E_1(\mathbf{k})$ and $E_2(\mathbf{k})$ with spin are given by

$$E_{1,2}(\mathbf{k})=\tfrac{1}{2}[\epsilon_1(\mathbf{k})+\epsilon_2(\mathbf{k})]\pm\tfrac{1}{2}\sqrt{[\epsilon_1(\mathbf{k})-\epsilon_2(\mathbf{k})]^2+4\lambda^2}\ . \tag{4.3}$$

TABLE II. Empirical matrix elements (in eV) for rhombohedral group-V semimetals.

	As	Sb	Bi
E_s	−10.277	−8.527	−9.643
E_p	−0.524	−0.294	−0.263
$V_{ss\sigma}$	−1.344	−0.923	−0.703
$V_{sp\sigma}$	1.275	1.170	1.300
$V_{pp\pi}$	−0.828	−0.658	−0.679
$V_{pp\sigma}$	2.857	2.340	2.271
$V'_{ss\sigma}$	−0.427	−0.366	−0.275
$V'_{sp\sigma}$	0.580	0.480	0.108
$V'_{pp\pi}$	−0.754	−0.534	−0.337
$V'_{pp\sigma}$	1.628	1.608	1.420
$V''_{ss\sigma}$	−0.004	0.000	−0.007
$V''_{sp\sigma}$	0.067	0.090	0.065
$V''_{pp\pi}$	−0.017	−0.040	0.004
$V''_{pp\sigma}$	0.55	0.210	0.303

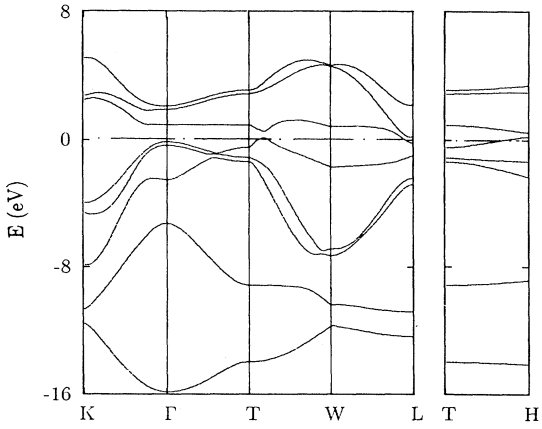

FIG. 3. Calculated band structure for As with spin-orbit coupling $\lambda=0.36$ eV.

This shows that the total energies are splitted by the spin-orbit coupling. Namely, the spin-orbit coupling leaves the degeneracy along the T-W line, leading to the conduction and valence bands being split along this line, remaining thus one below the Fermi level and the other above it all along the T-W line. On the other hand, the spin-orbit interaction alters only slightly the level structure along the T-H line, and the location of the hole pockets at H point is essentially unchanged. These details of the band structure for Sb agree well with pseudopotential calculation[13] and the *ab initio* results.[15]

For Bi, only the bands near the T and L points are close to the Fermi level. The slight overlap (at the T and L points) between valence and conduction bands is hardly visible. It can be noted in bismuth, where the spin-orbit coupling ($\sim$1.5 eV) is larger than most interaction parameters, from Fig. 5 that the maximum splitting induced by the spin-orbit interaction for the p bands is about 1.5 eV along the Γ-T line. In particular, the crossover point along the T-W line corresponding to the case without spin-orbit coupling is splitted and the location of

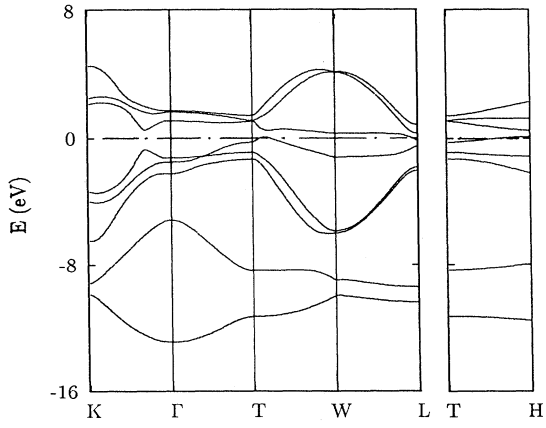

FIG. 4. Calculated band structure for Sb with spin-orbit coupling $\lambda=0.6$ eV.

TABLE III. Values of overlaps between conduction and valence bands, and the coordinates of the H point for As and Sb. (a) Difference between the Fermi energy and the extremal energy for electrons (in eV); (b) difference between the Fermi energy and the extremal energy for holes (in eV); (c) coordinates of the H point for As and Sb, expressed in trigonal coordinates.

	As	Sb	Bi
(a) Electrons:			
Present work	0.234	0.160	0.0259
Other theoretical	0.408,[a] 0.367[b]	0.206,[a] 0.115,[c] 0.108[d]	0.0183,[a] 0.016[c], 0.027[e]
Experimental	0.202,[f] 0.190[g]	0.093–0.160[f]	0.02–0.030[f,h]
(b) Holes:			
Present work	0.196	0.095	0.0144
Other theoretical	0.202,[a] 0.362[b]	0.114,[a] 0.119,[c] 0.142[d]	0.0234,[a] 0.008,[c] 0.012[e]
Experimental	0.154,[f] 0.177[g]	0.0844[f]	0.006–0.016[f,h]
(c) H point:			
Present work	(0.387,0.459,0.387)	(0.365,0.440,0.365)	
Other theoretical	(0.194,0.370,0.194)[a]	(0.163,0.350,0.163)[a]	
	(0.204,0.376,0.204)[b]	(0.101,0.372,0.101)[c]	
		(0.245,0.393,0.245)[d]	

[a]Reference 15.
[b]P. J. Lin and L. M. Falicov, Phys. Rev. **142**, 441 (1966).
[c]Reference 24.
[d]Reference 13.
[e]Reference 14.
[f]Reference 3.
[g]M. G. Priestley *et al.*, Phys. Rev. **154**, 671 (1967).
[h]V. S. Edel'man, Adv. Phys. **25**, 555 (1976).

hole pocket is pushed to the T point by the spin-orbit effect. This result is consistent with the pseudopotential[14] and first-principle[15] calculations.

In the three materials, the overlap between the conduction and valence bands creates free electrons at L, and free holes at H (for As and Sb) or T (for Bi). This overlap decreases from As to Sb to Bi: about 0.43 eV for As, 0.255 eV for Sb, and 0.04 eV for Bi. The magnitude and the location of these overlaps obtained from our tight-binding calculation are in good agreement with the first-principle calculation[15] and experimental results.[3]

The overlap values and the coordinates of the maxima of the valence band are summarized in Table III. The location of the free hole and electron pockets we find here is commonly accepted by other authors.[12–15,24] The spin-orbit coupling is very important in bismuth since, without it, the holes would not be obtained in the experimentally observed location point T.[3] The comparison of our band-structure calculations at the symmetry points, Γ, T, and L with the *ab initio* results[15] is given in Table IV. It can be noted that our results provide good valence bands and the overlaps between conduction and valence bands. In particular, the results for Bi and Sb are fairly accurate. The conduction bands are not well reproduced by our tight-binding method, which we attribute to the common problem faced by all the tight-binding-like approaches, that is, the conduction bands tend to be too flat.

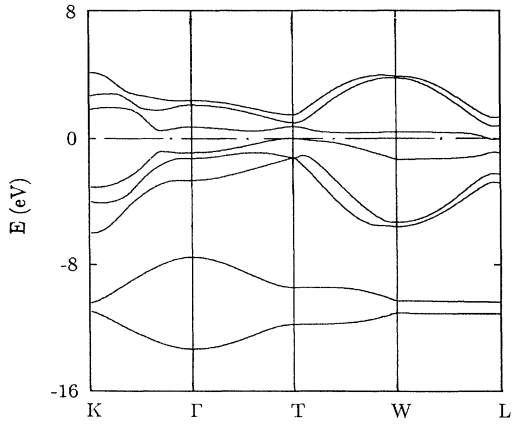

FIG. 5. Calculated band structure for Bi with spin-orbit coupling $\lambda = 1.5$ eV.

V. DISCUSSIONS AND CONCLUSION

We have developed a tight-binding theory for the rhombohedral group-V semimetals. Our approach is comparable with that proposed by Chadi and Cohen[7] and by Vogl, Hjalmarson, and Dow[8] for diamond and zinc-blende semiconductors. The interaction parameters have been determined based upon a two-center approximation for As, Sb, and Bi by fitting the existing pseudopotential and *ab initio* results. It can be seen from Table II that as far as the nearest- (next-nearest-) neighbors are concerned, all these parameters have the right signs for two-center integrals of the corresponding atomic orbitals, as well as the right order of magnitude: the largest interaction is $V_{pp\sigma}$ ($V'_{pp\sigma}$) between two p orbitals pointing along the bond, while $V_{ss\sigma}$ ($V'_{ss\sigma}$), the interaction of s orbitals, is considerably smaller, and the other interactions even

TABLE IV. Comparison of our results for the energies (in eV) of As, Sb, and Bi at the symmetry points Γ, T, and L with the *ab initio* calculations (Ref. 15).

	As		Sb		Bi	
Level	Ours	Ref. 15	Ours	Ref. 15	Ours	Ref. 15
Γ_6^+	−15.84	−15.10	−12.87	−12.67	−13.32	−13.01
Γ_6^-	−5.57	−5.22	−5.17	−4.89	−7.53	−7.28
Γ_6^+	−2.52	−2.57	−2.25	−2.28	−2.66	−2.73
Γ_6^+	−0.36	−1.89	−1.50	−1.55	−1.25	−0.80
Γ_{45}^+	−0.12	−1.67	−1.22	−1.28	−0.89	−0.61
Γ_6^-	0.94	1.61	1.08	1.87	0.72	1.11
Γ_6^-	1.90	2.89	1.64	2.56	2.11	3.33
Γ_{45}^-	2.12	2.94	1.74	2.98	2.41	3.63
T_6^-	−13.96	−13.56	−11.26	−11.11	−11.78	−11.55
T_6^+	−9.14	−10.00	−8.36	−8.89	−9.39	−9.67
T_6^-	−1.40	−1.91	−1.33	−1.50	−1.25	−1.67
T_{45}^-	−1.13	−1.56	−0.90	−1.00	0.014	0.023
T_6^+	−0.47	−0.44	−0.26	−0.33	−1.22	−1.28
T_6^+	0.92	0.67	1.06	0.09	0.77	0.49
T_{45}^+	2.89	1.01	1.09	0.39	1.50	1.33
T_6^-	3.13	2.11	1.41	1.31	1.00	1.11
L_s	−12.36	−12.22	−10.36	−10.22	−11.09	−11.00
L_a	−10.81	−11.00	−9.42	−9.56	−10.35	−10.28
L_s	−2.80	−2.88	−2.05	−2.06	−2.83	−2.01
L_a	−2.42	−2.61	−1.81	−1.83	−2.27	−1.99
L_s	−1.01	−0.56	−0.50	−0.39	−0.026	−0.018
L_a	−0.23	−0.41	−0.16	−0.21	−0.90	−0.28
L_s	0.13	0.21	0.28	0.28	0.83	0.76
L_a	2.17	1.50	0.84	0.72	1.36	1.33

smaller. As far as the third-nearest neighbors are concerned, the parameters are much smaller than the nearest- and next-nearest-neighbor terms. According to our calculations, we find that a reasonably approximate band structure for As, Sb, and Bi might be obtained by considering only the nearest- and next-nearest-neighbor interactions. However, in order to fit the fine structure of the pseudopotential and *ab initio* results, for instance, the level structures near the L point in three semimetals and near the H point in As and Sb, one has to include the third-nearest-neighbor terms. Detailed calculations show that the overlap along the W-L and T-H lines is very sensitive to the third-neighbor interactions $V''_{pp\sigma}$ and $V''_{pp\pi}$, while the other two third-neighbor interaction parameters $V''_{ss\sigma}$ and $V''_{sp\sigma}$ have little effect on the band structures. In practice, one can still get a fairly good result by neglecting $V''_{ss\sigma}$ and $V''_{sp\sigma}$.

Our calculations have shown that the spin-orbit coupling is very important in rhombohedral group-V semimetals. In the cases of As and Sb, this coupling leads to several specific degeneracies which affect directly the locations of hole pockets. In the case of Bi, this effect turns out to highly significant since, without it, the holes would not be obtained in the experimentally observed location. The only disadvantage of our calculations is attributed to the common problem faced by all the tight-binding-like methods, that is, the valence bands can be fit fairly well, but the conduction bands tend to be too flat (i.e., the electron effective massses tend to be too large). Besides this, the magnitude of the overlap between the conduction and valence bands and its location obtained from our tight-binding calculation are in good agreement with the pseudopotential and first-principle results, as well as with experimental data throughout.

As we mentioned in the Introduction, this work was motivated by the recent experiments on the semimetal-semiconductor heterostructures.[1,2] Our next goal is to use these tight-binding parameters determined for semimetals to study Sb/GaSb (111) and Bi/CdTe (111) heterostructures and superlattices.

ACKNOWLEDGMENTS

This research was supported by the Texas Center for Superconductivity at the University of Houston, a grant from the Robert A. Welch Foundation, and the Advanced Technology Program of the Texas High Education Coordinating Board under Grant No. 003652-228.

APPENDIX: EXPRESSIONS OF THE TIGHT-BINDING MATRIX ELEMENTS

$$H_{1s1s}=E_s+V''_{ss\sigma}\left[2\cos k_y+4\cos\frac{\sqrt{3}}{2}k_x\cos\frac{k_y}{2}\right], \tag{A1}$$

$$H_{1s1x}=i2\sqrt{3}V''_{sp\sigma}\sin\frac{\sqrt{3}}{2}k_x\cos\frac{k_y}{2}\ , \tag{A2}$$

$$H_{1s1y}=i2V''_{sp\sigma}\left[\sin k_y+\cos\frac{\sqrt{3}}{2}k_x\sin\frac{k_y}{2}\right]\ , \tag{A3}$$

$$H_{1s2s}=V_{ss\sigma}\left[e^{i\xi_1}+2\cos\frac{k_y}{2}e^{-i\eta_1}\right]+V'_{ss\sigma}\left[e^{-i\xi_2}+2\cos\frac{k_y}{2}e^{i\eta_2}\right]\ , \tag{A4}$$

$$H_{1s2x}=V_{sp\sigma}A_1\left[e^{i\xi_1}-\cos\frac{k_y}{2}e^{-i\eta_1}\right]-V'_{sp\sigma}A_2\left[e^{-i\xi_2}-\cos\frac{k_y}{2}e^{i\eta_2}\right]\ , \tag{A5}$$

$$H_{1s2y}=i\sqrt{3}V_{sp\sigma}A_1\sin\frac{k_y}{2}e^{-i\eta_1}+i\sqrt{3}V'_{sp\sigma}A_2\sin\frac{k_y}{2}e^{i\eta_2}\ , \tag{A6}$$

$$H_{1s2z}=-\sqrt{3}V_{sp\sigma}c_1A_1\left[e^{i\xi_1}+2\cos\frac{k_y}{2}e^{-i\eta_1}\right]+\sqrt{3}V'_{sp\sigma}c_2A_2\left[e^{-i\xi_2}+2\cos\frac{k_y}{2}e^{i\eta_2}\right]\ , \tag{A7}$$

$$H_{1x1x}=E_p+3V''_{pp\sigma}\cos\frac{\sqrt{3}}{2}k_x\cos\frac{k_y}{2}+V''_{pp\pi}\left[\cos\frac{\sqrt{3}}{2}k_x\cos\frac{k_y}{2}+2\cos k_y\right]\ , \tag{A8}$$

$$H_{1x1y}=-\sqrt{3}(V''_{pp\sigma}-V''_{pp\pi})\sin\frac{\sqrt{3}}{2}k_x\sin\frac{k_y}{2}\ , \tag{A9}$$

$$\begin{aligned}H_{1x2x}=&\tfrac{1}{2}V_{pp\sigma}A_1^2\left[2e^{i\xi_1}+\cos\frac{k_y}{2}e^{-i\eta_1}\right]+3V_{pp\pi}A_1^2c_1^2\left[e^{i\xi_1}+2\left[1+\frac{1}{4c_1^2}\right]\cos\frac{k_y}{2}e^{-i\eta_1}\right]\\&+\tfrac{1}{2}V'_{pp\sigma}A_2^2\left[2e^{-i\xi_2}+\cos\frac{k_y}{2}e^{i\eta_2}\right]+3V'_{pp\pi}A_2^2c_2^2\left[e^{-i\xi_2}+2\left[1+\frac{1}{4c_2^2}\right]\cos\frac{k_y}{2}e^{i\eta_2}\right]\ ,\end{aligned} \tag{A10}$$

$$H_{1x2y}=-\frac{\sqrt{3}}{2}(V_{pp\sigma}-V_{pp\pi})A_1^2\sin\frac{k_y}{2}e^{-i\eta_1}+\frac{\sqrt{3}}{2}(V'_{pp\sigma}-V'_{pp\pi})A_2^2\sin\frac{k_y}{2}e^{i\eta_2}\ , \tag{A11}$$

$$H_{1x2z}=-\sqrt{3}(V_{pp\sigma}-V_{pp\pi})c_1A_1^2\left[e^{i\xi_1}-\cos\frac{k_y}{2}e^{-i\eta_1}\right]-\sqrt{3}(V'_{pp\sigma}-V'_{pp\pi})c_2A_2^2\left[e^{-i\xi_2}-\cos\frac{k_y}{2}e^{i\eta_2}\right]\ . \tag{A12}$$

$$H_{1y1y}=E_p+V''_{pp\sigma}\left[\cos\frac{\sqrt{3}}{2}k_x\cos\frac{k_y}{2}+2\cos k_y\right]+3V''_{pp\pi}\cos\frac{\sqrt{3}}{2}k_x\cos\frac{k_y}{2}\ , \tag{A13}$$

$$\begin{aligned}H_{1y2y}=&\tfrac{3}{2}V_{pp\sigma}A_1^2\cos\frac{k_y}{2}e^{-i\eta_1}+V_{pp\pi}\left[6A_1^2(c_1^2+\tfrac{1}{4})\cos\frac{k_y}{2}e^{-i\eta_1}+e^{i\xi_1}\right]\\&+\tfrac{3}{2}V'_{pp\sigma}A_2^2\cos\frac{k_y}{2}e^{i\eta_2}+V'_{pp\pi}\left[6A_2^2(c_2^2+\tfrac{1}{4})\cos\frac{k_y}{2}e^{i\eta_2}+e^{-i\xi_2}\right]\ ,\end{aligned} \tag{A14}$$

$$H_{1y2z}=-i3(V_{pp\sigma}-V_{pp\pi})c_1A_1^2\sin\frac{k_y}{2}e^{-\eta_1}-i3(V_{pp\sigma}-V_{pp\pi})c_2A_2^2\sin\frac{k_y}{2}e^{\eta_2}\ , \tag{A15}$$

$$H_{1z1z}=E_p+V''_{pp\pi}\left[2\cos k_y+\cos\frac{\sqrt{3}}{2}k_x\cos\frac{k_y}{2}\right]\ , \tag{A16}$$

$$\begin{aligned}H_{1z2z}=&3V_{pp\sigma}c_1^2A_1^2\left[e^{i\xi_1}+2\cos\frac{k_y}{2}e^{-i\eta_1}\right]+V_{pp\pi}A_1^2\left[e^{i\xi_1}+2\cos\frac{k_y}{2}e^{-i\eta_1}\right]\\&+3V'_{pp\sigma}c_2^2A_2^2\left[e^{-i\xi_2}+2\cos\frac{k_y}{2}e^{i\eta_2}\right]+V'_{pp\pi}A_2^2\left[e^{-i\xi_2}+2\cos\frac{k_y}{2}e^{i\eta_2}\right]\ ,\end{aligned} \tag{A17}$$

where

$$\xi_{1,2}=\frac{\sqrt{3}}{3}k_x-c_{1,2}k_z \ , \tag{A18}$$

$$\eta_{1,2}=\frac{\sqrt{3}}{6}k_x+c_{1,2}k_z \ , \tag{A19}$$

and

$$A_{1,2}=\frac{1}{1+3c_{1,2}^2} \ . \tag{A20}$$

[1]T. J. Golding, J. A. Dura, W. C. Wang, J. T. Zborowski, A. Vigliante, J. H. Miller, and J. R. Meyer, Semicond. Sci. Technol. **8**, S117 (1993).
[2]A. Divenere, X. J. Xi, C. L. Hou, J. B. Ketterson, G. K. Wong, and I. K. Sou, Appl. Phys. Lett. (to be published).
[3]J. P. Issi, Aust. J. Phys. **32**, 585 (1979), and references therein.
[4]J. R. Meyer, F. J. Bartoli, E. R. Youngdale, and C. A. Hoffman, J. Appl. Phys. **70**, 4317 (1991).
[5]J. C. Slater and G. F. Koster, Phys. Rev. **94**, 1498 (1954).
[6]W. A. Harrison, *Electronic Structure and the Properties of Solids* (Freeman, San Francisco, 1980).
[7]D. J. Chadi and M. L. Cohen, Phys. Status Solidi **68**, 405 (1975).
[8]P. Vogl, H. P. Hjalmarson, and J. D. Dow, J. Phys. Chem. Solids **44**, 365 (1983).
[9]J. N. Schulman and Y. C. Chang, Phys. Rev. B **24**, 4445 (1981); **27**, 2346 (1983).
[10]S. Mase, J. Phys. Soc. Jpn. **13**, 434 (1958); **14**, 584 (1959).
[11]M. H. Cohen, L. M. Falicov, and S. Golin, IBM J. Res. Develop. **8**, 215 (1964).
[12]L. M. Falicov and S. Golin, Phys. Rev. **137**, A871 (1965).
[13]L. M. Falicov and P. J. Lin, Phys. Rev. **141**, 562 (1966).
[14]S. Golin, Phys. Rev. **166**, 643 (1968).
[15]X. Gonze, J. P. Michenaud, and J. P. Vigneron, Phys. Rev. B **41**, 11 827 (1990).
[16]D. Weaire and M. F. Thorpe, Phys. Rev. B **4**, 2508 (1971).
[17]D. Liberman, J. T. Waber, and D. T. Cromer, Phys. Rev. **137**, A27 (1965).
[18]R. J. Needs, R. M. Martin, and O. H. Nielsen, Phys. Rev. B **33**, 3778 (1986).
[19]J. Donohue, *The Structures of the Elements* (Wiley, New York, 1974).
[20]M. H. Cohen, Phys. Rev. **121**, 387 (1961).
[21]C. S. Barrett, P. Cucka, and K. Haefner, Acta. Crystallogr. **16**, 451 (1963).
[22]P. Cucka and C. S. Barrett, Acta Crystallogr. **15**, 865 (1962).
[23]P. O. Löwdin, J. Chem. Phys. **18**, 365 (1950).
[24]J. Rose and R. Schuchardt, Phys. Status Solidi B **117**, 213 (1983).